High impact cast sheets of poly(methyl methacrylate) with low levels of polyurethane

Ph. Heim*, C. Wroteckiâ€ , M. Avenel and P. Gaillard
Elf Atochem, Groupement de Recherches de Lacq, BP 34, 64170 Artix, France
(Received 3 March 1992)

High impact strength, high transparency cast sheets of polyurethane (PU)-reinforced poly(methyl methacrylate) (PMMA) were obtained by means of IPN techniques. The PU content was kept low (less than 10%). The impact strength is maximum at a critical PU concentration, and for a given morphology. The study of various synthesis parameters led to the conclusion that the size of interstitial PMMA nodules – and therefore the optical and mechanical properties of the final material – are determined by the crosslink density of the swollen PU network at the onset of the methyl methacrylate polymerization.

(Keywords: interpenetrating polymer network; poly(methyl methacrylate); polyurethane cast sheets; impact)

INTRODUCTION

A classical way of increasing the impact resistance of poly(methyl methacrylate) (PMMA) is by dispersing elastomeric latex particles within the PMMA matrix. This process is very satisfactory for the production of high impact PMMA sheets by extrusion; however, impact resistance is poor when the sheets are cast[1].

The interpenetrating polymer network (IPN) technique allows two different polymer networks formed *in situ* in the mould to be combined to a limited extent by mixing all monomers and precursors before casting (one-shot process). High impact strength, transparent PMMA cast sheets could be obtained by this IPN technique. Firstly, an elastomeric polyurethane (PU) network is obtained by polycondensation at room temperature in the presence of methyl methacrylate (MMA), followed by high temperature free-radical polymerization of the MMA contained in the swollen elastomeric network.

The basic IPN principles were described by Frisch and Sperling in the late 1960s[2–4]. The key parameters determining the morphology, and hence the mechanical properties of the final material, are the relative rates of formation of the two networks[5–10]. Correlation of the relative rates of network formation with the size of the phase-separated domains has, however, often led to contradictory results. Some authors recommend simultaneous formation[6], whereas others favour the sequential process[7–11]. In fact, each IPN case must be considered individually since the degree of compatibility between the two polymers, the crosslink densities and the relative composition must be taken into account.

The various studies concerning PU/PMMA IPNs have recently been reviewed by Hur *et al.*[12]. Excellent quality high impact materials were obtained by Allen *et al.*[13–18], but most of them had a PU content of greater than 20%. They also found that the size of PMMA domains varies from a few micrometres to a few nanometres with increasing PU concentration. The thermomechanical spectra generally exhibit two transitions, but also indicate a limited macromolecular interaction between PU and PMMA phases; it is likely that this interaction occurs at the interface. Meyer *et al.*[9,10,19–23] concentrated their attention on the chemical aspects of the synthesis and the effects of the kinetics of formation of both networks. Fox *et al.*[24] have also recommended sequential network formation in order to obtain transparent materials.

In general the elastic modulus increases with the extent of phase interpenetration[25]. The characteristics of the first crosslinked network determine the domain size of the second polymer, which is in turn responsible for the damping properties of the IPN[26]. Various studies have similarly concluded that grafting the two networks improves the optical and mechanical properties, due to an improved phase interpenetration[27,28].

In most of the papers reviewed, the influence of the PU concentration was studied in the range 0% to 100% but by intervals of 10%; there is an almost linear relationship between PU content and mechanical properties. Our investigation focused on the 0–20% PU range; it was found that within this range there is a critical PU concentration which gives optimum impact strength. This paper is a summary of the synthesis and characterization of these so-called 'PU/PMMA IPNs'. Our main aim was to explain the influence of many of the synthesis process parameters, and to correlate them to the properties and morphologies of the final materials.

* To whom correspondence should be addressed
† Present address: Cray Valley, BP 19, 62320 Drocourt, France

0032-3861/93/081653-08

EXPERIMENTAL

The characteristics of the reagents used are summarized in *Table 1*. The MMA was dried on a molecular sieve. The hydroxyl compounds and the isocyanates were titrated once a month according to French Standard NFT 52132 in order to know the exact concentration of reactive moieties. The final formulation was obtained by mixing two previously degassed component solutions A and B. The mixture was poured into a mould made from two glass plates measuring 300 × 300 mm and sealed by means of a PVC gasket; this allowed a 4 mm thick cast sheet to be obtained. After filling, the mould was immersed horizontally in a water bath at 60°C for 5 h, then cured in an air-circulating oven for 2 h at a temperature higher than 100°C. Methacrylic solution A contained the components for the PU network and the initiators for the MMA; methacrylic solution B contained the acrylic crosslinking agent and the catalyst for the PU network. The levels of PU catalyst used enabled all the ingredients to be mixed in the same vessel without gelation for at least 1 h, provided the PU concentrations were less than 10%.

For example, in order to obtain a PMMA plate with a PU content of 6%: solution A containing 46 parts MMA, 4.91 parts T2000 diol, 1.09 parts N100 triisocyanate, 0.018 parts V40, 0.036 parts AIBN and 0.018 parts V65 was mixed with solution B containing 46 parts MMA, 0.45 parts DBTL and 1.5 parts DMEG. For this mixture the NCO/OH molar ratio is 1.2. I.r. kinetic measurements have shown that with this type of PU catalysis and MMA initiators, the PMMA network begins to form before the PU network is completed.

Some of the experiments, pointed out in the text, were conducted without the V65 low temperature initiator. In this case the MMA polymerization starts later, and the PU network has time to be virtually completely converted.

Mechanical measurements

Unnotched Charpy impact. According to French standard NFT 51035, sample 4 mm thick, 10 mm wide, 40 mm span, CEAST instrument. Unreinforced PMMA: 11 kJ m^{-2}.

Table 1 Materials used

Code	Materials	Source
MAM	Methyl methacrylate without stabilizer	Atochem
DMEG	Diethyleneglycol dimethacrylate	Atochem
Terathane T2000	Polytetramethylene glycol (diol); molecular weight, 2000; 9.8×10^{-4} mol OH/g	DuPont
Desmodur N100	Hexamethylene diisocyanate trimer; % NCO, 22.2; 5.29×10^{-3} mol NCO/g	Bayer
HMDI	Hexamethylene diisocyanate; 1.19×10^{-2} mol NCO/g	
DBTL	Stannous dibutyldilaurate, purity 85%	Ciba-Geigy
V65	2,2′azobis(2,4-dimethylvaleronitrile); T 1/2, 10 h at 51°C in toluene	WACO
V40	1,1′azobis(cyclohexane-1 carbonitrile); T 1/2; 10 h at 88°C in toluene	WACO
AIBN	2,2′azobis isobutyronitrile; T 1/2; 10 h at 65°C in toluene	SFOS

Notched Izod impact tests. According to ISO 180 standard, Zwick apparatus. Specimen 70 × 12.7 × 4 mm, notch length 2.7 mm. Unreinforced PMMA: 0.7 kJ m^{-2}.

Flexural modulus. According to ISO R378, Instron 1185 machine with 80 × 10 × 4 mm cut specimen. Span length 66 mm. Crosshead speed 2 mm min^{-1}. Unreinforced PMMA: 3300 MPa.

Thermomechanical measurements

A Rheometrics DRS770 apparatus was used between −130°C and +250°C under rectangular torsion loading geometry, heating rate 2°C min^{-1}, at a frequency of 1 Hz.

Electron microscopy

Two methods were tested in order to study the morphology of our materials.

Scanning electron microscopy (SEM). A plane surface was cut at room temperature, by means of an ultramicrotome, from a sample taken in the centre of a cast sheet. The sample was then subjected to carbon and gold metallization, and observed under low voltage (5 kV). Since the PU and PMMA phases deform differently when being cut, they can be distinguished on the micrographs, the PMMA being darker.

Transmission electron microscopy (TEM). Although this technique is more delicate to perform it gives excellent results. Microslices 80 nm thick were cut by an ultramicrotome, placed on a copper grid and treated with ruthenium tetroxide vapour for 30 min. A very good contrast between the two phases is obtained; the PMMA appears white and the polyurethane black.

Optical measurements

An Interlab Colorquest spectrophotometer was used to determine the light transmittance of 40 × 40 × 4 mm samples at 710 nm.

RESULTS

The following synthesis parameters were studied: PU content; relative formation kinetics of the two networks, as a function of the DBTL catalyst concentration (for the PU) and the type of initiator (for the PMMA); and crosslink density of the PU network, controlled by the tri/diisocyanate (N100/HMDI) NCO molar ratio.

The effect of these parameters on the mechanical, thermomechanical, morphological and optical properties will be described below.

Mechanical properties

Effect of PU content. Figures 1 and *2* present the unnotched Charpy and notched Izod impact strength respectively, as a function of the PU content (4 to 22%) for sheets with the same composition as the example given above. Unexpectedly an anomalous point appears on both curves, where for a critical PU content of about 6% the impact resistance is equal to that obtained with a 20% PU content. In addition, there is a very good compromise between impact strength and modulus in the case of low PU content (2200 MPa flexural modulus for 6% PU *versus* 1500 MPa for 20% PU).

Figure 3 shows the variations of unnotched Charpy

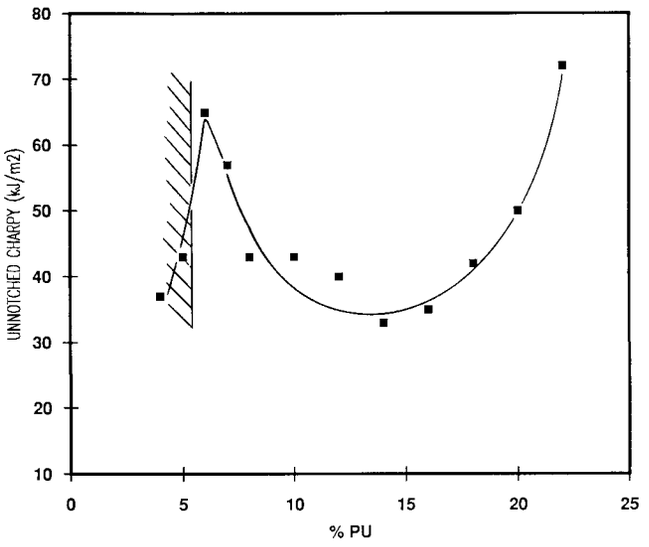

Figure 1 Variation of unnotched Charpy impact strength of PU/PMMA IPN as a function of PU content (molar ratio NCO/OH = 1.2; DBTL 0.45%/sheet; with V65)

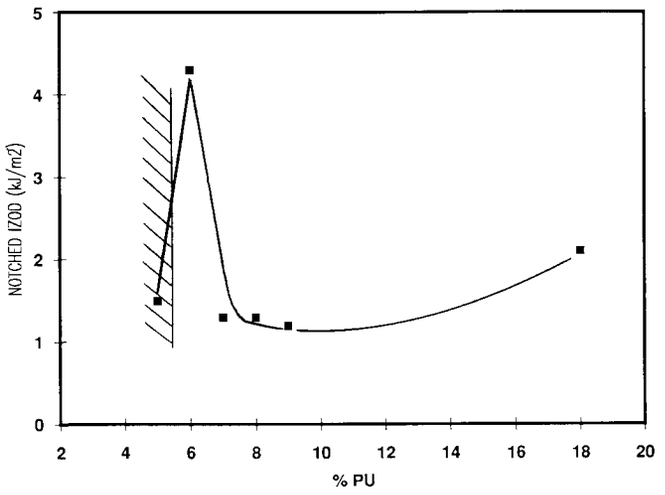

Figure 2 Variation of notched Izod impact strength of PU/PMMA IPN as a function of PU content (molar ratio NCO/OH = 1.2; DBTL 0.45%/sheet; with V65)

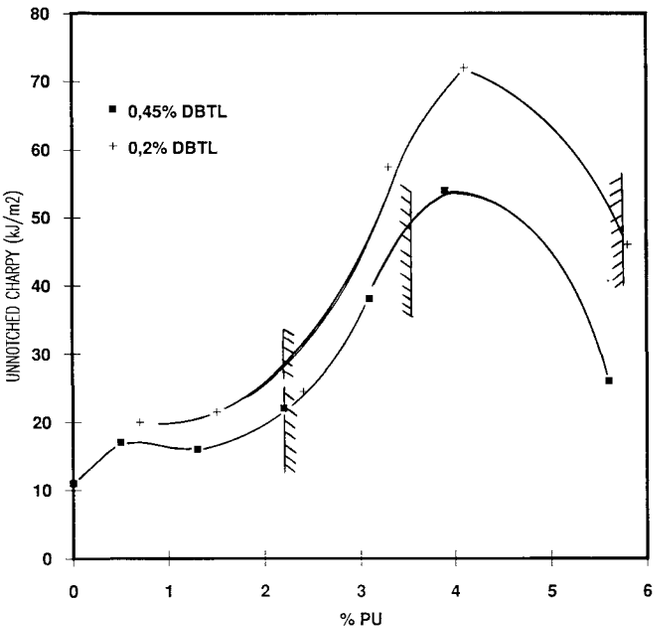

Figure 3 Variation of unnotched Charpy impact strength of PU/PMMA IPN as a function of PU content (two different DBTL levels; 0.2% and 0.45%/sheet; molar ratio NCO/OH = 1.7; without V65)

impact strength as a function of PU content (0.5–6%), for two different PU catalyst concentrations. In this case, the low temperature V65 initiator was omitted. Again and also unexpectedly, the curves exhibit an anomalous point, located this time between 3 and 5% PU.

Effect of the relative rate of formation of the two networks. The polymerization of the PMMA network can be delayed by eliminating the low temperature V65 initiator. The effect of this parameter on impact resistance can be examined by comparing *Figures 1* and *3*: the anomalous point moves towards lower PU contents as the PMMA polymerization is delayed. In addition, the rate of formation of the polyurethane network can be slowed down by reducing the DBTL catalyst concentration. *Figure 4* shows the typical variation of the unnotched Charpy impact strength and the modulus as a function of DBTL content for a PU content of 18%. It can be seen that impact resistance increases with decreasing quantities of DBTL whereas the modulus varies in the opposite manner.

Similar variations are obtained for other PU concentrations, including for the anomalous point. *Figure 3* illustrates one example.

Effect of the tri/diisocyanate (N100/HMDI) NCO molar ratio. The influence of the PU crosslink density has been examined by varying the ratio between di- and triisocyanate. The results given in *Table 2* show that the impact strength increases and the modulus and transparency decrease as the triisocyanate is replaced by diisocyanate (see also *Figure 5*). These variations are greater in the case of higher PU content.

Mechanical measurements

Figures 6 and *7* show the changes in G', G'' and $\tan\delta$ for the two materials at 6% and 18% PU, the impact strength of which is given in *Figure 1*. The spectra for 5% and 7% PU are similar. All the curves have the same shape, with two significant transitions: (1) at high temperature (120–130°C) – the glass transition of the PMMA phase, the value of which corresponds to a

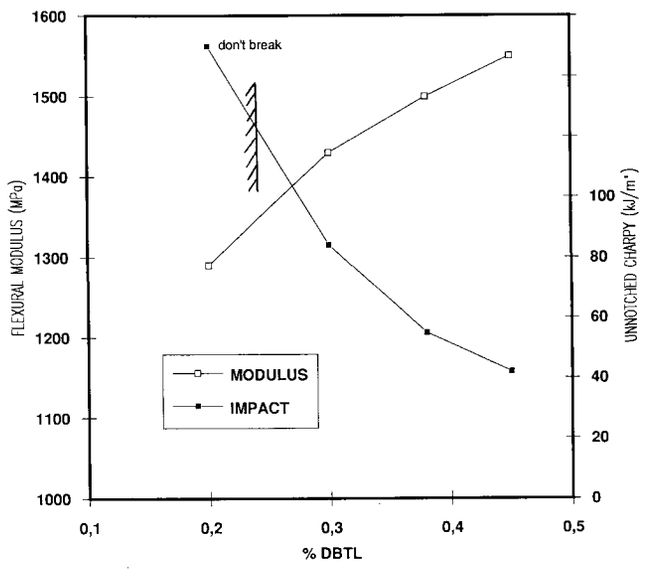

Figure 4 Variation of unnotched Charpy impact strength and modulus as a function of PU catalyst (DBTL) content (PU 18%; molar ratio NCO/OH = 1.2; with V65)

Table 2 Mechanical and optical properties as a function of molar NCO ratio tri/diisocyanate (molar ratio NCO/OH = 1.2; DBTL 0.38%/sheet; with V65)

	NCO mole ratio				
% PU	N100	HMDI	Unnotched Charpy ($kJ\,m^{-2}$)	Flexural modulus (MPa)	Light transmission at 710 nm (%)
7	100	0	57	2200	90
	83	17	72	2040	88
	75	25	80	2020	87
	50	50	89	–	73
18	100	0	55	1550	92
	75	25	70	1460	91
	50	50	105	1330	89
	5	95	Unbroken	1000	75

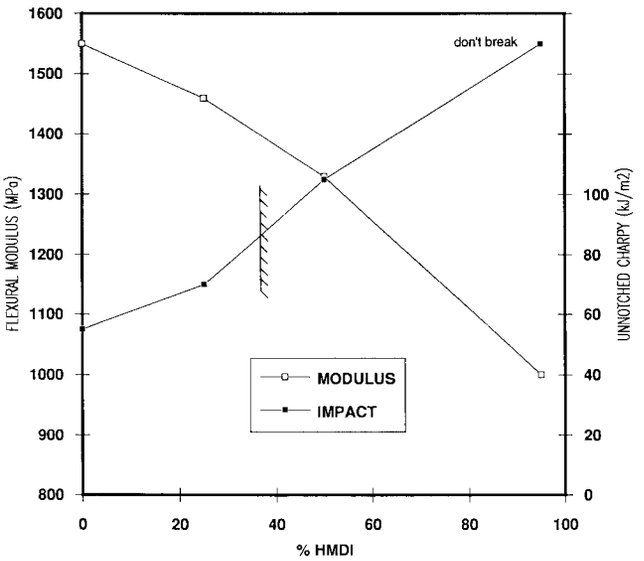

Figure 5 Variation of mechanical properties as a function of molar NCO ratio tri/diisocyanate (PU 18%; molar ratio NCO/OH = 1.2; DBTL 0.38%/sheet; with V65)

crosslinked PMMA; (2) at low temperature (−60°C to +5°C) – the secondary β transition of the PMMA and the glass transition of the PU, which is concealed by this very wide PMMA β transition.

A slight shift in the glass transition of the PMMA with the PU content can be noted (130°C for 5% PU, 120°C for 18% PU).

Morphological characterization

The scanning electron micrographs of *Figure 8* and transmission electron micrographs of *Figure 9* show that the structure of the materials consists of large PMMA nodules 0.5 to 10 μm in size embedded in a PU/PMMA IPN, to the left of the anomalous point (see *Figures 1* and *3*). To the right of the anomalous point the size of the nodules decreases as the PU content increases until the phase interpenetration is such that the nodules are no longer visible. For PU contents as high as about 20%, and under the conditions detailed in the Experimental section, the materials appear totally homogeneous despite the fact that thermomechanical measurements still indicate two separate glass transitions. When the PU content is low, below 3%, the structure consists of PU fragments dispersed in PMMA.

Figure 10 is a micrograph showing the morphology of a 7% PU sheet obtained with a 50/50 di/triisocyanate NCO molar ratio. The size of PMMA nodules is considerably larger than in *Figure 8d*.

Optical properties

The transparency limit is indicated on all curves showing the variations of impact strength as a function of various synthesis parameters. The plates are cloudy on the hatched side of this limit, and transparent on the other side. As a general rule the plates are cloudy to the left of the irregular point, and clear to the right. The refraction index of the pure PU phase at 20°C was measured to be 1.478. The PMMA refraction index at 20°C was 1.49. The transparency of the sheets is directly linked to the size of the PMMA nodules and to the difference in the refraction index between the two phases[29] and to the temperature. The sheets begin to be cloudy when the size of nodules exceeds about 1 μm.

DISCUSSION

Our study has shown that cast sheets of transparent and high impact strength PMMA are obtained by polymerizing MMA within a more or less completely crosslinked PU network. Such sheets have been obtained in the past[13,14], but only with a high PU content of about 20%. Detailed examination of the 0–20% PU range has revealed the existence of an anomalous point for impact strength at a critical PU concentration. This irregular point occurs between 3 and 7% PU depending on the synthesis conditions. At this critical concentration, the impact strength (as measured by unnotched Charpy and notched Izod tests) is as high as that obtained with a PU content of 20% (see *Figures 1* and *2*).

Morphological characterization has allowed the conclusion that the structure of the material at the irregular point consists of PMMA nodules 0.2 to 1 μm in size embedded in a more or less continuous PU-rich matrix. *Figure 1* shows that beyond the critical PU content, these nodules disappear rapidly to give a material with a structure of highly interpenetrated networks. The impact strength first decreases, and then increases again due to the rising PU concentration. Just to the left of the anomalous point, very large nodules are found (1–10 μm

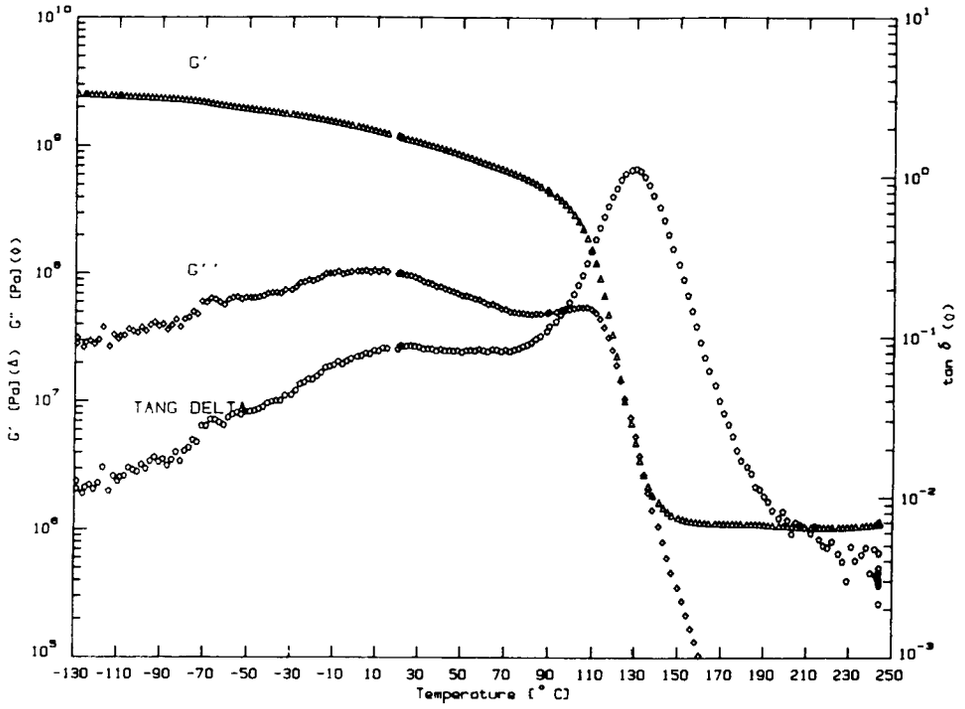

Figure 6 Dynamic mechanical loss measurements for PU/PMMA IPN with 6% PU

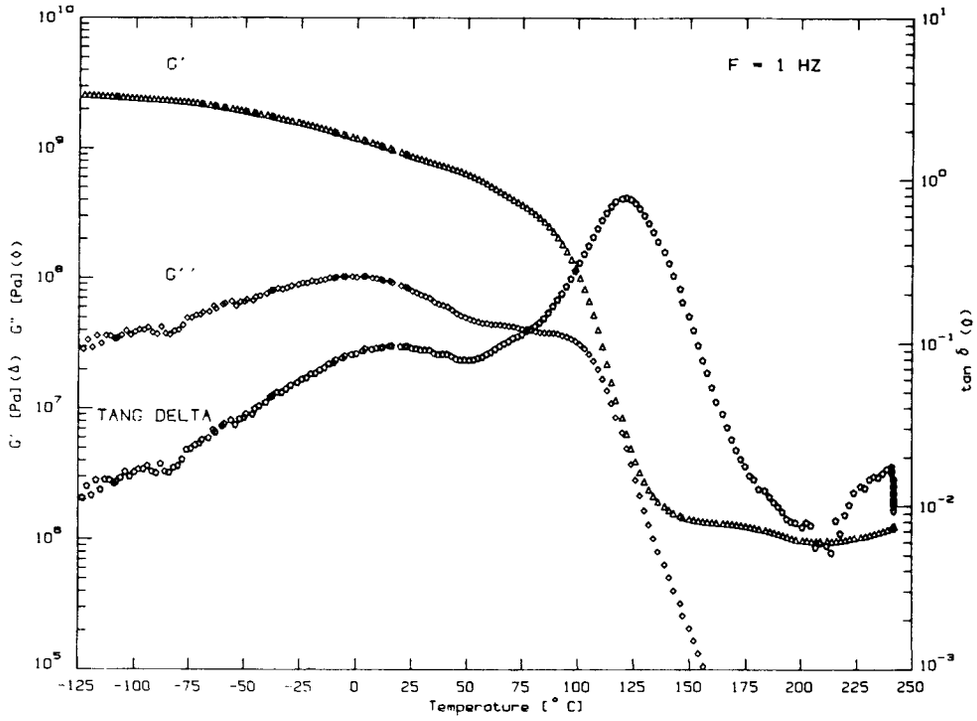

Figure 7 Dynamic mechanical loss measurements for PU/PMMA IPN with 18% PU

or more); these large dimensions adversely affect the impact strength and the transparency of the material. *Table 3* and *Figure 9* show that for very low PU contents (less than 3%), the structure of the material consists of PU fragments dispersed in PMMA; this type of structure provides no impact reinforcement. The size of the PU fragments determines the transparency of the sheets.

Thermomechanical measurements have shown that, whatever the PU content, there are always two phases even when there is a large interpenetration of the two networks. The shifting of the PMMA glass transition towards lower temperatures with increasing PU content indicates, however, that molecular interactions occur to a larger extent in this case, inducing a larger interphase volume. No conclusions can be drawn regarding the PU glass transition, which is very weak anyway, since it is hidden by the PMMA β transition. We wish to explain why a particular size of nodule is formed, or indeed why in some cases no nodules are formed at all. Examination of the different synthesis parameters merely

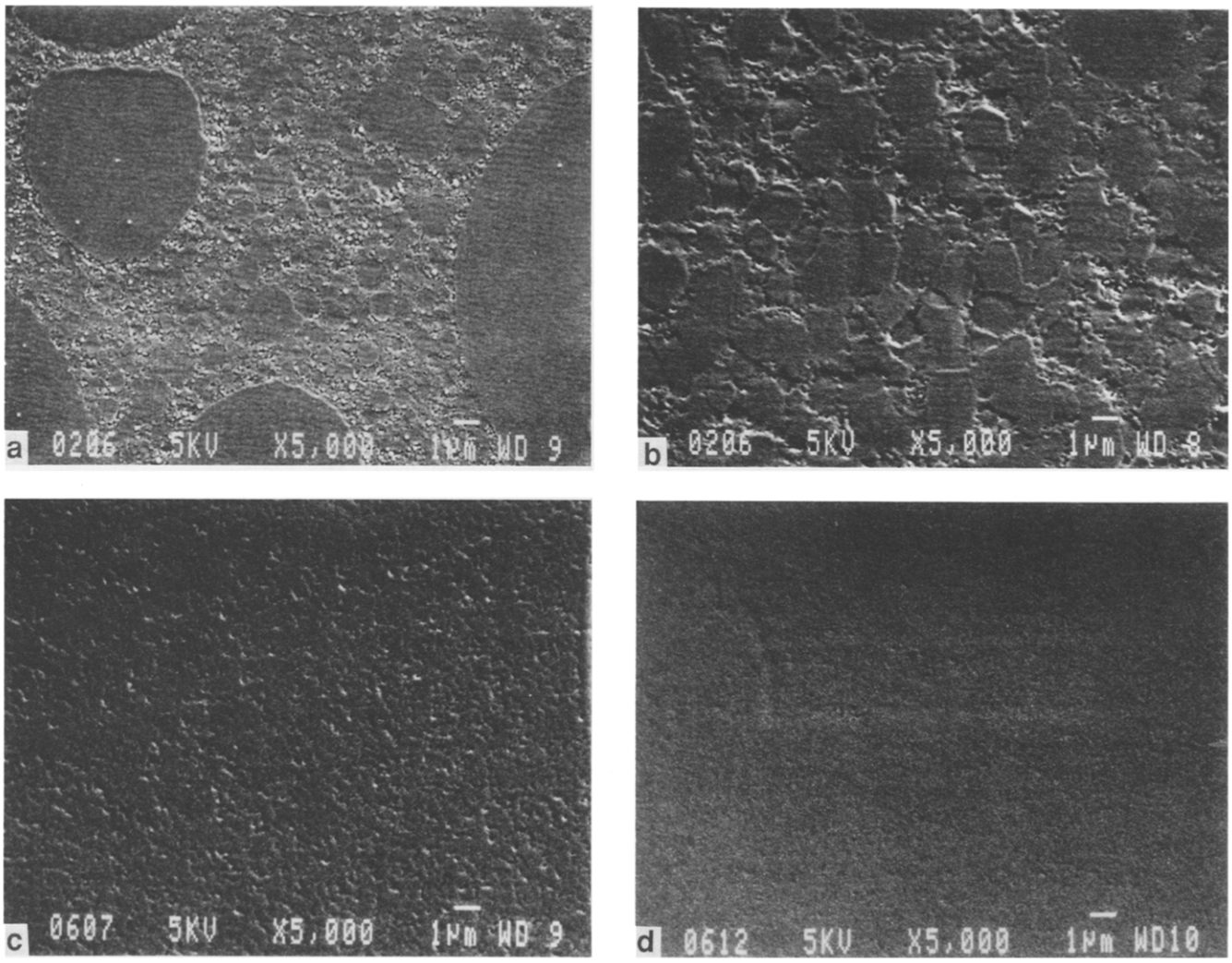

Figure 8 SEM micrographs of PU/PMMA IPN (DBTL 0.45%/sheet; molar ratio NCO/OH = 1.2; with V65): (a) 4% PU; (b) 5% PU; (c) 6% PU; (d) 7% PU

confirms our opinion that the size of the interstitial PMMA nodules is determined by the crosslink density of the swollen PU network at the onset of the MMA polymerization. The greater this crosslink density, the more the structure of the material tends towards that of a true IPN. However, if the polyurethane network is poorly converted, or if the distance between crosslinks is large at the beginning of the MMA polymerization, the material will have a nodular structure. The fewer crosslinks contained in the PU network, the greater will be the size of these nodules. Thus any parameter acting on this crosslink density will also modify the morphology. The morphological results of *Table 3* can be summarized as follows: for PU contents of less than 3%, the concentration of PU-forming reagents is so small that the network cannot be completely crosslinked in the available space; when the MMA begins to polymerize, more or less branched polyurethane chains cluster into domains dispersed within the PMMA, because of the thermodynamic incompatibility between the two polymers. Subsequently the crosslink density of the network will increase with the PU concentration. It occupies the whole volume as a gel, thus leading to interstitial polymerization of the MMA; therefore the PU constitutes the continuous phase, whereas the size of the PMMA nodules will decrease to finally disappear as the PU crosslink density increases.

The shifting of the anomalous point observed between *Figures 1* and *3* can be explained simply: eliminating the V65 initiator caused the MMA polymerization to begin later compared with the formulations of *Figure 1*. In this case the PU network will have time to be completed and the PMMA nodules generated will be smaller. In order to obtain the critical 0.2 to 1 μm nodule size, less PU must be used, thus shifting the anomalous point to lower PU contents.

Furthermore it was verified that generating PMMA nodules in the case of the 18% PU IPN of *Figure 1* considerably increases the impact strength, to the detriment of the modulus. One way of generating such nodules, or of increasing their size, is either to decrease the concentration of PU catalysts (see *Figure 4*) in order to have a lower degree of conversion, and hence lower crosslinking at the start of MMA polymerization, or to use increasing quantities of diisocyanate to achieve the same result (see *Figure 5*). The different morphologies obtained with and without diisocyanate for 7% PU IPNs are clearly visible on the micrograph of *Figure 10* and *Figure 8d*.

Other parameters, such as the polymerization

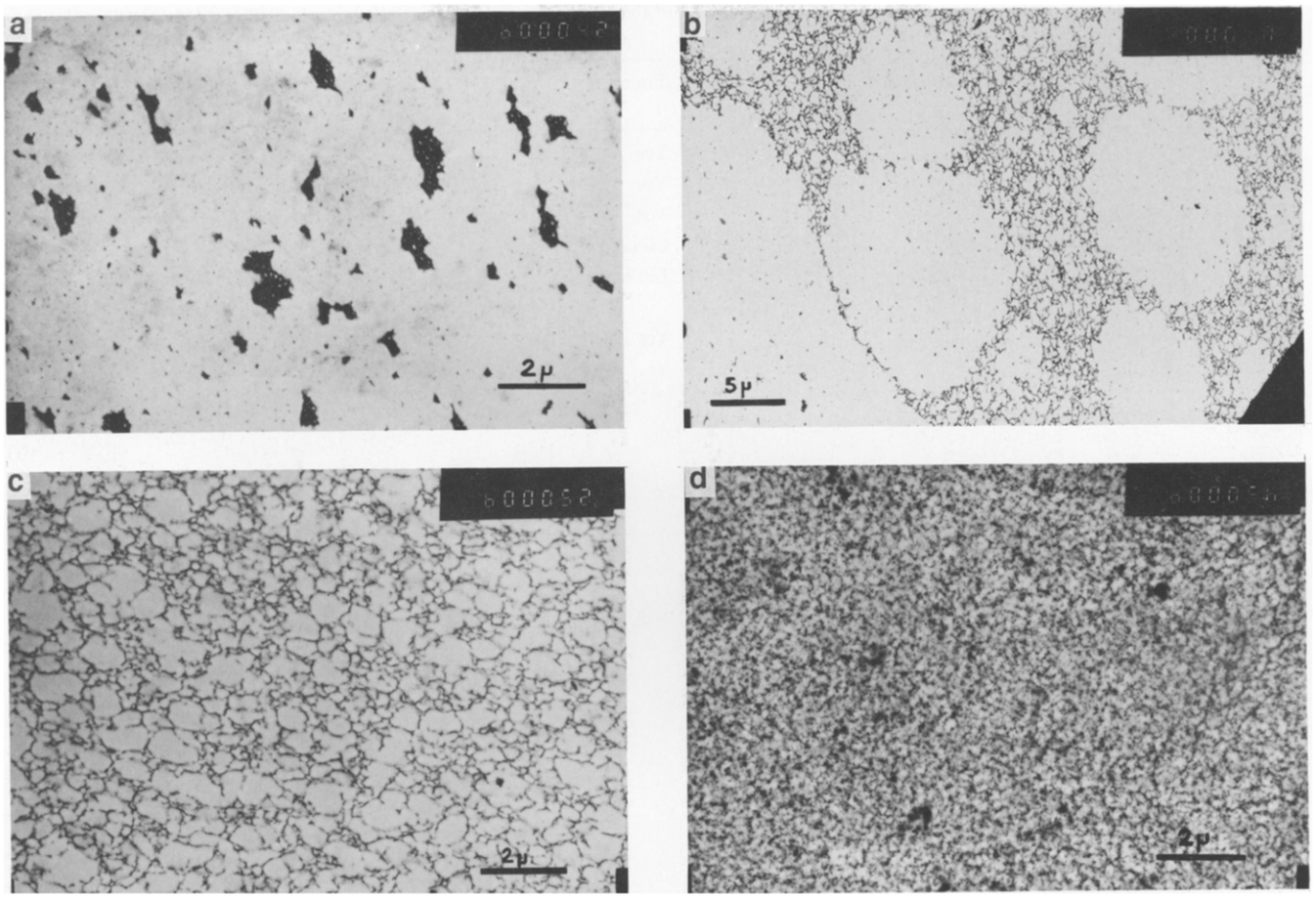

Figure 9 TEM micrographs of PU/PMMA IPN (DBTL 0.45%/sheet; molar ratio NCO/OH = 1.7; without V65): (a) 2.2% PU; (b) 3.1% PU; (c) 3.9% PU; (d) 5.6% PU

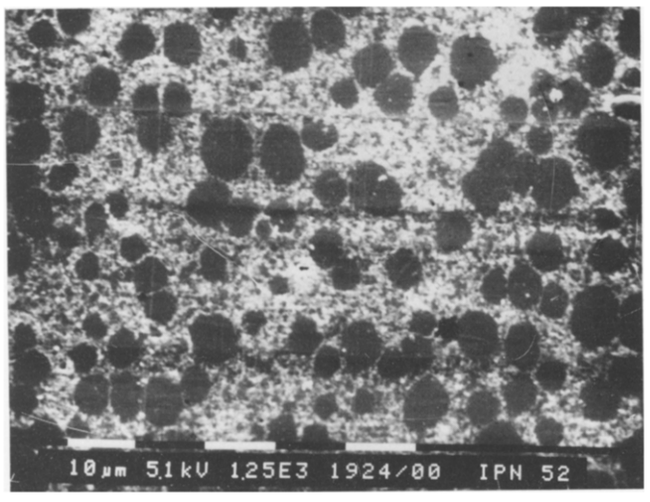

Figure 10 SEM micrograph of PU/PMMA IPN with 7% PU and molar NCO ratio tri/diisocyanate of 50/50

temperature cycle, the NCO/OH ratio, the nature and molecular weight of the PU precursors, also affect the crosslink density of the swollen PU. The effect of these parameters will not be developed in this paper.

CONCLUSION

Improving the impact strength of cast sheets of PMMA with PU by the IPN technique was studied. It has been found that an optimum impact strength can be achieved with a small PU content (between 3% and 7%). This lower PU content provides a very good compromise between modulus and impact strength, much better in fact than that for sheets containing 20% PU which exhibit the same impact resistance. This optimum is obtained when the structure of the material consists of PMMA nodules approximately 0.2 to 1 μm in size dispersed within a more or less continuous PU matrix.

The study of the influence of various synthesis parameters correlated with the mechanical properties and the morphology has led to the conclusion that the size of the interstitial PMMA nodules is determined by the crosslink density of the swollen PU network at the start of MMA polymerization. It has been shown that the morphology of the material is changed by any parameter modifying this crosslink density. In particular, we have examined the role of the concentration of PU catalyst, the di/triisocyanate ratio, the PU content and the PMMA initiator system. Altering these parameters allows the critical PU concentration corresponding to the anomalous point to be changed. The transparency of the sheets obtained is always correlated to the size of PMMA nodules.

Future work will include first a more detailed characterization of the nature of the interphase and the continuity of the various phases, and secondly a study of the fracture mechanisms of these materials as a function of the morphology. In addition, future work will also

Table 3 Mechanical and optical properties and morphology of PU/PMMA IPN as a function of PU content (DBTL 0.45%/sheet; molar ratio NCO/OH = 1.7;without V65)

% PU	Unnotched Charpy ($kJ\,m^{-2}$)	Transparent	Morphology by TEM
0	11	Yes	
0.5	17	Yes	Fragments of PU (~0.05 μm in PMMA)
1.3	16	Yes	As above
2.2	22	Cloudy	As above but (~1.2 μm)
3.1	38	Little haze	Large PMMA nodules (~10–15 μm) in IPN PU/PMMA
3.9	54	Yes	PMMA nodules (~0.2–1 μm) in PU
5.6	26	Yes	Interpenetration

include the study of such parameters as internetwork grafting and crosslinking.

Finally, we have shown that the impact strength cannot be improved by merely increasing the PU content as in the case of extruded high impact PMMA reinforced with fixed morphology latex particles. All the synthesis parameters acting on the crosslink density of the swollen PU network at the onset of MMA polymerization must be accurately adjusted in order to obtain the desired morphology.

REFERENCES

1 ICI, Eur. Pat. Appl. EP 297706
2 Frisch, H. L., Klempner, D. and Frisch, K. C. *J. Polym. Sci., Part B* 1969, **7**, 775
3 Sperling, L. H. and Friedman, D. W. *J. Polym. Sci., Part A2* 1969, **7**, 425
4 Sperling, L. H. 'Interpenetrating Polymer Networks and Related Materials' Plenum Press, New York, 1981
5 Kim, S. C., Klempner, D., Frisch, K. C., Frisch, H. L. and Radigan, W. *Macromolecules* 1976, **9**, 258
6 Touhsaent, R. E., Thomas, D. A. and Sperling, L. H. *J. Polym. Sci., Polym. Symp.* 1974, **46**, 175
7 Lee, J. H. and Kim, S. C. *Macromolecules* 1986, **19**, 644
8 Devia, N., Manson, J. A., Sperling, L. H. and Conde, A. *Macromolecules* 1979, **12**, 360
9 Djomo, H., Widmaier, J. M. and Meyer, G. C. *Polymer* 1983, **24**, 1415
10 Tabka, M. T., Widmaier, J. M. and Meyer, G. C. *Macromolecules* 1989, **22**, 1826
11 Devia-Manjarres, N., Manson, J. A., Sperling, L. H. and Conde, A. *Polym. Eng. Sci.* 1978, **18**, 200
12 Hur, T., Manson, J. A., Hertzberg, R. W. and Sperling, L. H. *J. Appl. Polym. Sci.* 1990, **39**, 1933
13 Allen, G., Bowden, M. J., Blundell, D. J., Hutchinson, F. G., Jeffs, G. M. and Vyvoda, J. *Polymer* 1973, **14**, 597
14 Allen, G., Bowden, M. J., Blundell, D. J., Jeffs, G. M., Vyvoda, J. and White, T. *Polymer* 1973, **14**, 604
15 Allen, G., Bowden, M. J., Blundell, D. J. and Jeffs, G. M. *Polymer* 1974, **15**, 13
16 Allen, G., Bowden, M. J., Blundell, D. J. and Jeffs, G. M. *Polymer* 1974, **15**, 19
17 Allen, G., Bowden, M. J., Blundell, D. J. and Jeffs, G. M. *Polymer* 1974, **15**, 28
18 Allen, G., Bowden, M. J., Blundell, D. J. and Jeffs, G. M. *Polymer* 1974, **15**, 33
19 Jin, S. R., Widmaier, J. M. and Meyer, G. C. *Polymer* 1988, **29**, 346
20 Jin, S. R., Widmaier, J. M. and Meyer, G. C. *Polym. Commun.* 1988, **29**, 26
21 Jehl, D., Widmaier, J. M. and Meyer, G. C. *Eur. Polym. J.* 1983, **19**, 597
22 Hermant, I. and Meyer, G. C. *Eur. Polym. J.* 1984, **20**, 85
23 Meyer, G. C. *Makromol. Chem., Rapid Commun.* 1983, **4**, 221
24 Fox, R. B., Bitner, L., Hinkley, J. A. and Carter, W. *Polym. Eng. Sci.* 1985, **25**, 157
25 Xiao, H. X., Frisch, K. C. and Frisch, H. L. *J. Polym. Sci., Polym. Chem. Edn* 1983, **21**, 2547
26 Shi, Y. and Nie, X. *Chim. J. Polym. Sci.* 1988, **6**, 244
27 Kircher, K., Mrotzek, W. and Menges, G. *Polym. Eng. Sci.* 1984, **24**, 974
28 Edison Polymer Innovation Corporation, Eur. Pat. Appl. EP 398490, 1990
29 Haaf, F., Breuer, H. and Echte, A. *J. Sci. Ind. Res.* 1981, **40**, 659